Stellar Associations in M51 and NGC 4214

Catherine Kaleida[1](kaleida@asu.edu), P. Scowen[1], B. Whitmore[2], R. Chandar[3], H. Kim[1], D. Calzetti[4], R. A. Windhorst[1], & WFC3 SOC team

[1]Arizona State University, [2]STScI, [3]Univ. of Toledo, [4]UMASS

M51 / NGC 5195 – Hubble WFC/ACS Optical: B, V, and I broadband and Hα

Mapping the Recent Star Formation History of the Disk of M51

We have conducted a photometric study of the stellar associations across the entire disk of the galaxy in order to assess trends in size, luminosity, and local environment associated with recent star formation activity in the system. Starting with a sample of over 900 potential associations, we produced color-magnitude and color-color diagrams for the 120 associations that were deemed to be single-aged. It has been found that main sequence turnoffs are not evident for the vast majority of the stellar associations in our set, potentially due to the overlap of isochronal tracks at the high mass end of the main sequence, and the limited depth of our images at the distance of M51. In order to obtain ages for more of our sample, we produced model spectral energy distributions (SEDs) to fit to the data from the GALEXEV simple stellar population (SSP) models of Bruzual & Charlot (2003). These SEDs can be used to determine age, size, mass, metallicity, and dust content of each association via a simple chi-squared minimization to each association's *BVI*-band fluxes. The derived association properties are mapped as a function of location, and recent trends in star formation history of the galaxy are explored in light of these results. This work is the first phase in a program that will compare these stellar systems with their environments using ultraviolet data from GALEX and infrared data from Spitzer, and ultimately we plan to apply the same stellar population mapping methodology to other nearby face-on spiral galaxies.

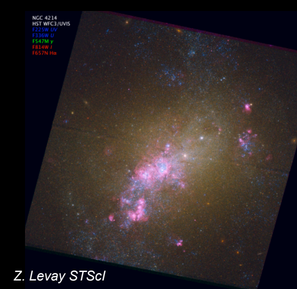

NGC 4214– Hubble WFC3/UVIS

The Size Scale of Stellar Groupings in NGC 4214

We investigate the sizes of stellar groupings in the nearby face-on spiral galaxy NGC 4214, using the Early Release Science (ERS) images from the Hubble Space Telescope Wide Field Camera 3 (*HST* WFC3). The currently available WFC3 data for NGC 4214 provides images in a range of wavelengths from ultraviolet to near-infrared, and at a high enough resolution (~0.6 pc/pixel) to discern individual stars. We aim to measure the size distribution of stellar groupings in this galaxy, in sizes ranging from stellar complexes (~200+ pc) to compact clusters (~3 pc), as well as their spatial distribution within the system. We have developed a uniform method of selecting stellar groups of various sizes, using Source Extractor (Bertin & Arnouts 1996) on a set of Gaussian-blurred images. The size of each selected cluster/association is then assessed by plotting the annular surface brightness as a function of radius, and taking the total radius of the stellar grouping to be where the surface brightness is 25% higher than the background. We will use the results from these methods to determine if there are preferred scales of clustering or if stars cluster continuously on all size scales.

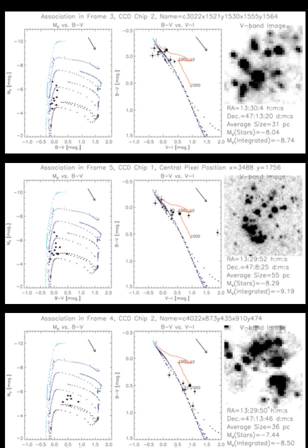

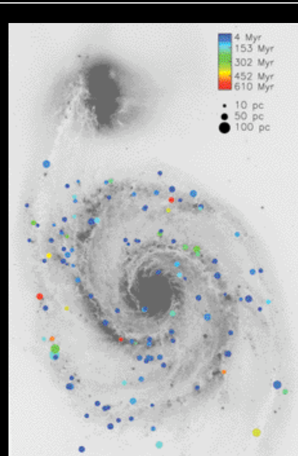

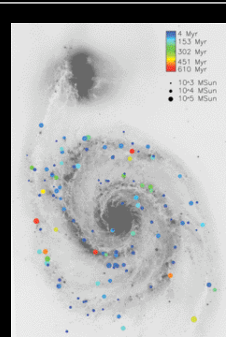

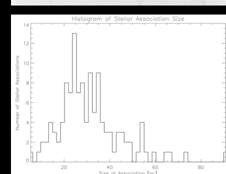

Selection of Stellar Associations/Clusters: We use Source Extractor on Gaussian blurred versions of the F547M image of NGC 4214. Images below are blurred with Gaussians of σ=5, 25, 50,75, and 100 pc .

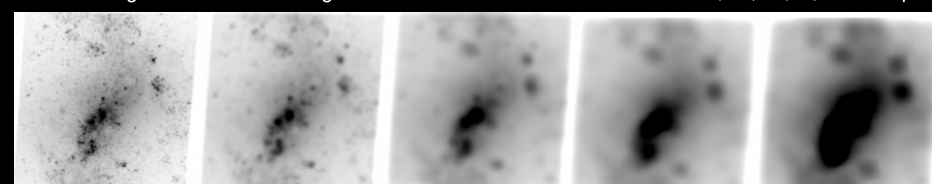

Determination of Association Sizes: R_{Total} (shown in red) is taken to be where the annular surface brightness is 25% larger than the background. Green reference circles mark r=50, 100, 150, and 200 pc.

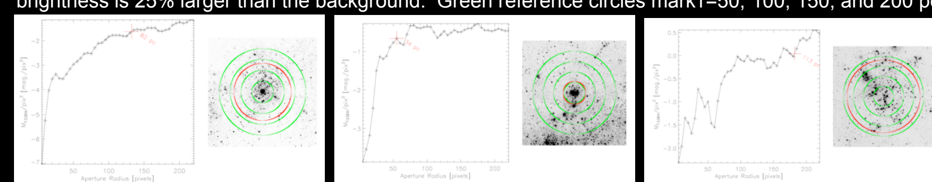

C.C. Kaleida & P.A. Scowen Aug. 2010 *The Astronomical Journal* **140** 379

This work was supported by NASA/STScI Grant HST-AR 1068401A to Arizona State University.

Support for program #11360 was provided by NASA through a grant from the Space Telescope Science Institute, which is operated by the Association of Universities for Research in Astronomy, Inc., under NASA contract NAS 5-26555.

The Transit Ephemeris Refinement and Monitoring Survey (TERMS)

Stephen R. Kane[1], David Ciardi[1], Debra Fischer[2], Greg Henry[3], Andrew Howard[4], Eric Jensen[5], Greg Laughlin[6], Suvrath Mahadevan[7], Kaspar von Braun[1], Jason Wright[7]

[1] NASA Exoplanet Science Institute, Caltech, MS 100-22, 770 South Wilson Avenue, Pasadena, CA, 91125, USA
[2] Department of Astronomy, Yale University, New Haven, CT, 06520, USA
[3] Center of Excellence in Information Systems, Tennessee State University, 3500 John A. Merritt Blvd, Nashville, TN, 37209, USA
[4] Department of Astronomy, University of California, Berkeley, CA, 94720, USA
[5] Department of Physics & Astronomy, 500 College Ave, Swarthmore College, Swarthmore, PA, 19081, USA
[6] UCO/Lick Observatory, University of California, Santa Cruz, CA, 95064, USA
[7] Department of Astronomy & Astrophysics, Pennsylvania State University, 525 Davey Laboratory, University Park, PA, 16802, USA

The Science Goals of TERMS

- Exploring the mass-radius relationship of exoplanets
- Calculating and refining transit ephemerides for the known RV planets
- Photometric monitoring of host stars during transit windows

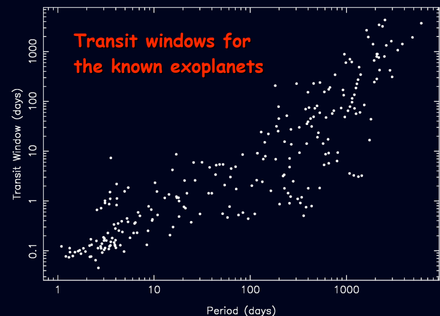

- We achieve the needed 1-2 millimags precision (shown below, WASP-5b)

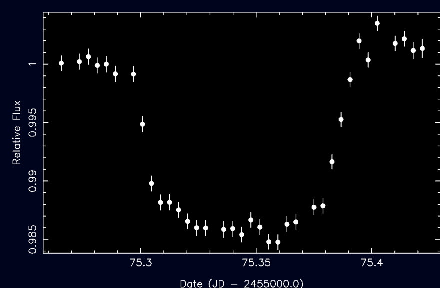

Results from TERMS

TERMS telescopes:

- CTIO 0.9m
- CTIO 1.0m (pictured - top)
- LCO 1.0m
- Keck/HIRES (pictured - bottom)
- APT (Fairborn Observatory)
- UCO/Lick 3.0m
- Hobby-Eberly Telescope
- Swarthmore College 24 inch

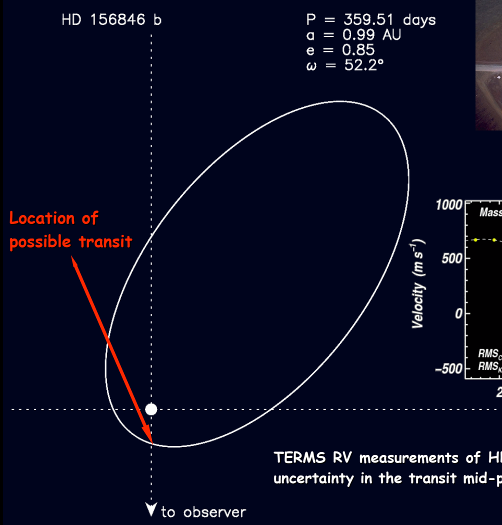

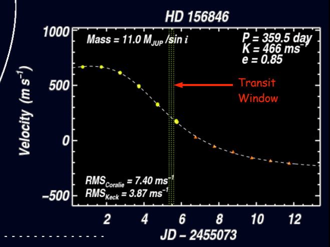

TERMS RV measurements of HD 156846 b resulted in an uncertainty in the transit mid-point of only 20 minutes!!

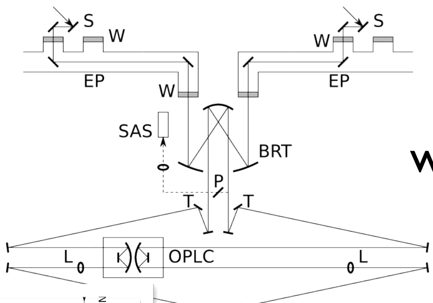

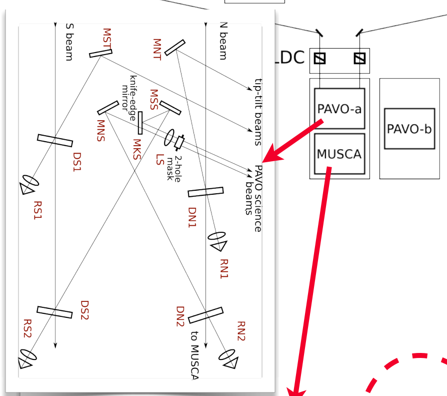

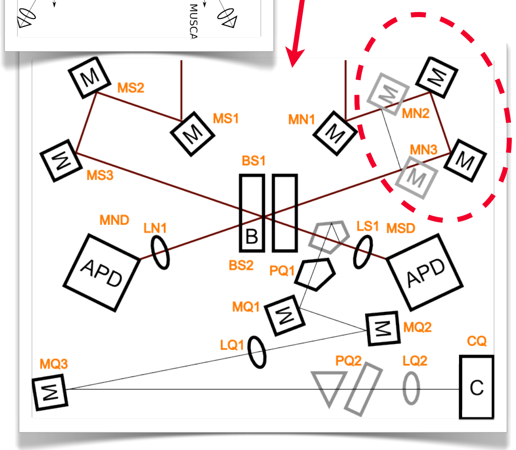

exoplanets

THE UNIVERSITY OF SYDNEY

with **M**icro-arcsecond **U**niversity of **S**ydney **C**ompanion **A**strometry

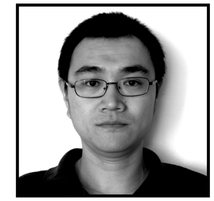

MUSCA Vitals	**Value**
Astrometry λ	0.81 — 0.95 μm
Fringe-tracking λ	0.53 — 0.81 μm
Tip-tilt λ	< 0.53 μm
Metrology λ	0.543 & 0.632 μm
FOV	~10"
Astrometric Resolution	~10 μas

- ★ MUSCA; new beam combiner in the making
- ★ Very narrow angle astrometry
- ★ Target resolution of 10μas
- ★ Search for planets around binary stars

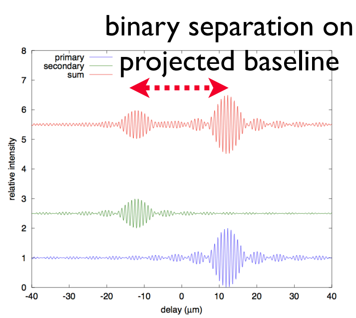

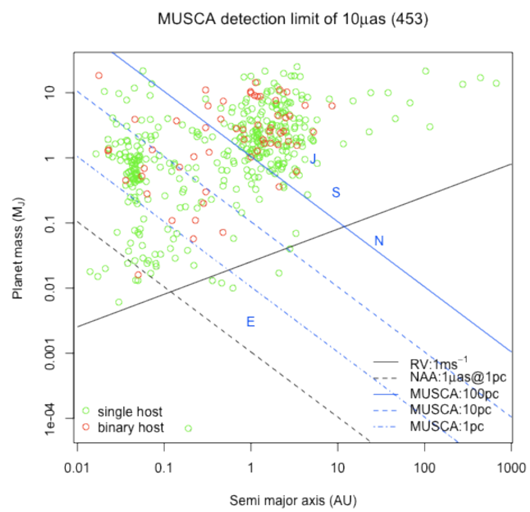

- ★ PAVO* as fringe tracker
- ★ MUSCA to measure separation of binary system
- ★ Targets:
  - ★ ~2$M_\odot$ stars
  - ★ ~M_J planets

SUSI% Vitals	**Value**
Orientation	N-S
Baselines	5, 10, 15, 20, 55, 60, 80, 110, 120, 160 m
Beam combiners	PAVO, *MUSCA*
Latitude	30° 19' S
Longitude	149° 33' E
Altitude	210m

*Precision Astronomical Visibility Observation
%Sydney University Stellar Interferometer

High-Resolution Ground-Based Transmission Spectroscopy of Exoplanetary Atmospheres

Adam Jensen

Wesleyan University

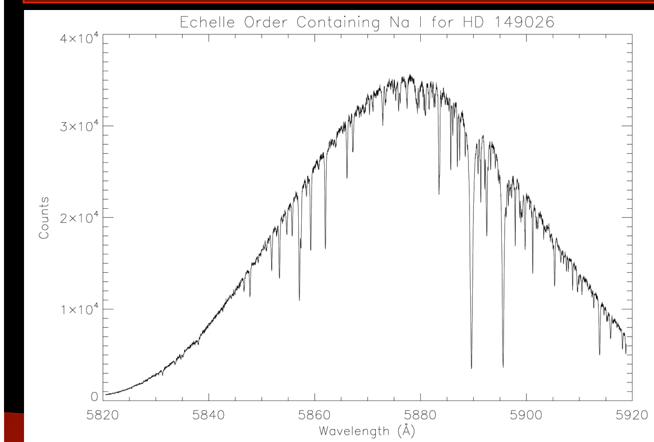

Above: Sample spectrum of the region covering Na I for one of our targets

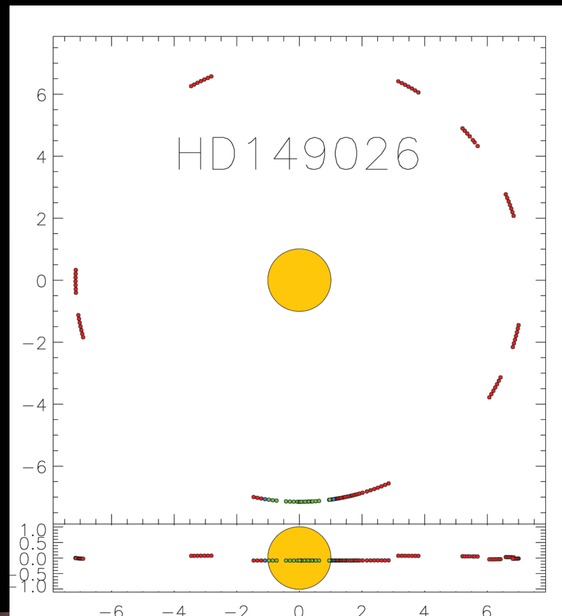

Above: Observations of HD 149026, scaled to stellar radius

Observations:
- •4 hot Jupiters and 1 hot Neptune
- •Hobby-Eberly Telescope's HRS @ R~60,000
- •600s exposures
- •Per target: 100+ total and 20+ in transit exposures

Program Goals
- •Find alkali metal lines (e.g. Na I, K I)
- •Characterize entire atmospheric spectra

Program Status
- •Data pipeline complete, spectra reduced and extracted
- •Currently analyzing
- •Expect Na I and/or K I results soon

Debris disk: a first view of extrasolar planetary systems

Jérémy Lebreton, Jean-Charles Augereau et al., *Université de Grenoble / Laboratoire d'AstrOphysique de Grenoble*

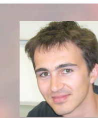

Context

• **Debris Disks** are a type of circumstellar disks, revealed by their infrared emission in ~20% of the MS stars.
• Extrasolar analogues to the Solar System **Edgeworth-Kuiper Belt**, they are the remnant of planet formation.

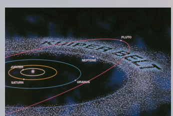

The Edgeworth-Kuiper Belt (EKB)
• A ~17 AU-wide disk of rocky and icy material extending beyond the orbit of Neptune (30 AU).
• From ~µm dust grains to >1000 km plutinos
• >70,000 EKB objects over 100 km
• Expected IR-excess $L_{dust}/L^* \sim 10^{-7}$

• These dusty disks differ from protoplanetary disks as they need to be continuously replenished through **collisions in a population of larger bodies.**
→ Asteroids, comets and planetesimals

The 500-meter asteroid Itokawa

Collisional cascade

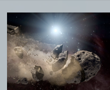

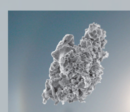

~10 µm dust grain

Key questions

• *We want a complete view of planetary systems and their history.*
• *Presence of exo-EKBs vs. presence of planets*
• *Elucidate the evolutionary link between gas-rich protoplanetary disks and gas-poor debris disks*
• *Investigate water abundances in the planet-forming regions of disks*

Disks and planets

• The presence of a companion imprints its signature on a debris disk
→ Clumps, rings, belts, eccentric distributions, spiral patterns, ...

Detailed modeling of these disks can reveal the position and mass of hidden planets.

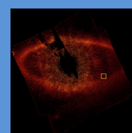

The offset between Fomalhaut and its disk is caused by a $<3M_J$ planet. (Kalas et al. 2008, *Science* **322**)

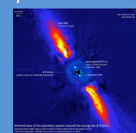

The planet in the disk of β Pictoris explains its ring-like structure and inner warp. (Lagrange et al. 2010, Science **329**, Absil et al. 2010, submitted to A&A)

• *How can asteroid belts affect habitability?*

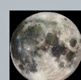

• ***The Late Heavy Bombardment**: In the young history (700 Myr) of the Solar System, the migration of giant planets pertubed the Kuiper Belt, bringing numerous planetesimals to hyperbolic orbits and resulting in a cataclysmic event on the primordial Earth.*

• *This event: (1) likely cleared a large fraction of the asteroids and comets of the Solar System **reducing the frequency of cataclysmic events** in its later history, (2) might have brought **large quantities of water onto the Earth surface.***

Earth-like planets with a comparable impact rate to the Earth may be uncommon!

Herschel observations and modeling of planetary systems around nearby stars

• Planetary systems as seen by Herschel
→ An ESA sub-mm Space Observatory with important participation from NASA

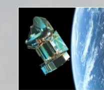

***GASPS**: GAS in Protoplanetary Systems (400h)*
Study of the transition gas-rich protoplanetary through gas-poor debris disks. PACS observations of fine structures lines ([CII], [OI],H_2O) for circumstellar disks down to ~10^{-5} M_{sun}.

HD 181327 *(Lebreton et al., in prep.)*

•*A young F5.5V star, member of the β Pictoris moving group (~12 Myr), located at 50.6 pc, with a far-IR excess $L_{IR}/L_* = 2.10^{-3}$.*
•*HST imaging of that debris disk revealed a 36 AU-wide ringlike disk centered at 86 AU.*

→The disk is cold (<88 K) and massive (0.2 $M_⊕$)
→The grains are porous aggregates (P ~ 65%) and contain a large fraction of ice (70%).
→They are small (amin~1µm) and close to collisional equilibrium.
→Non-detection of the [OI] and [CII] lines

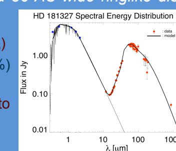

***DUNES**: DUst around NEarby Stars (140h)*
PACS and SPIRE photometric observations of cold disks around nearby stars. Characterization of faint « exo-Kuiper Belts » ($L_{dust}/L_* \sim$ a few times 10^{-7})

q¹ Eri *(Augereau et al., in prep.)*

•*A ~2 Gyr-old solar-type star (F8V), located at 17 pc. $L_{IR}/L_* = 3.8.10^{-4}$.*
•*The disk is **resolved in both scattered and thermal light**, revealing a ~40 AU wide belt peaking at ~85 AU.*
→ « The first real Edgeworth-Kuiper Belt analogue ever observed »
•*The initial disk mass inferred from a collisional approach is unrealistically high → Recent perturbation? Delayed stirring by a yet undiscovered planet?*

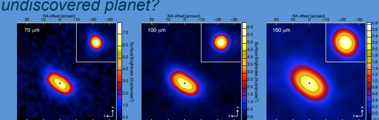

Herschel/PACS images of the q1 Eri disk at 70, 100 and 160 µm

Stellar Variability in Planetary Transit Searches

Amy McQuillan (University of Oxford)

Variability on hours timescales:
… causes detection problems for long period planets.
… introduces errors on derived system parameters.

Want to characterize variability as function or stellar properties, using methods such as:

AutoRegressive Moving Average (ARMA) Models

$$x_t = \sum_{i=1}^{p} \varphi_i x_{t-i} + \sum_{j=1}^{q} \theta_i \omega_{t-i} + \omega_t + c$$

Component	Timescale B (hr)
Active regions	2800 to 8300
Super-granulation	8 to 19
Meso-granulation	2.2
Granulation	0.05 to 0.14
Bright points	0.02

Example: Power spectrum of the PMO6 total solar irradiance light curve (1996-2001), showing a multi-component AR fit (from Aigrain et al 2004, A&A, 414, 1139).

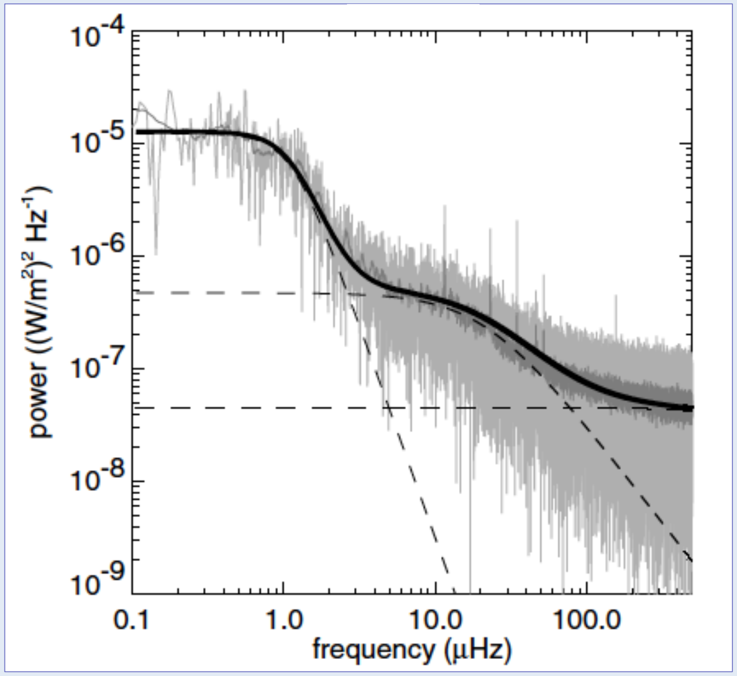

Adaptive optics & high-contrast imaging

Katie Morzinski  Center for Adaptive Optics ◆ UC Santa Cruz

I. Experiments with MEMS deformable mirrors

- Broad influence function limits mid-to-high-spatial-frequency stroke:
  - 70-cm-pitch woofer mitigates saturation on 8-m Gemini to 4-5 σ
  - Contributed to selection of the Gemini Planet Imager woofer
- MEMS for open-loop control:
  - Sub-nm stability, position repeatability, & hysteresis
  - Phase-to-volts MEMS model
- Open-loop control works as well as closed-loop:
  - ViLLaGEs on-sky AO testbed at Lick Obs. 1-m Nickel telescope
  - Visible-λ MEMS-AO

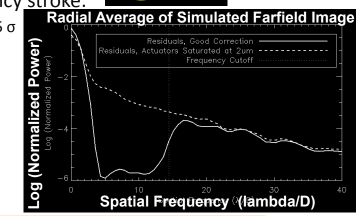

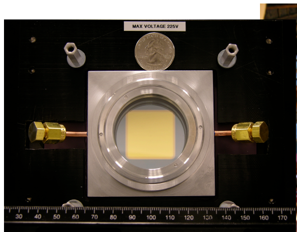

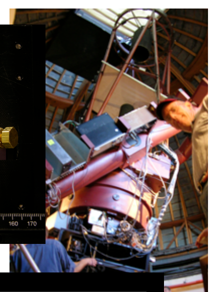

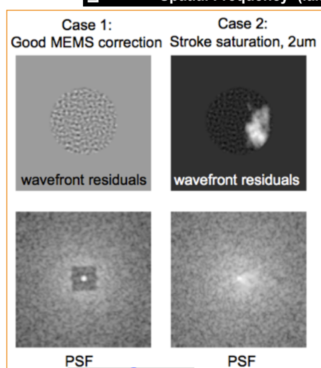

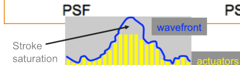

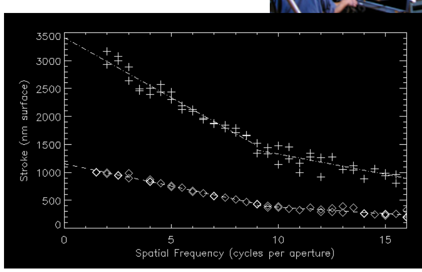

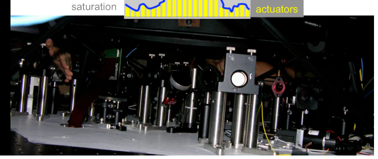

II. LOCI high-contrast imaging survey for faint companions (through brown dwarfs) to solar-type stars

- NGS AO deep imaging in near-IR
  - Keck-10m and Lick-3m, 2005-2009
  - Epoch 1: 88 main-sequence Hyades stars
  - Epoch 2: ~40 binaries & BD candidates
  - Probing 5-230 AU
  - Mass limit: ~0.02 $M_\odot$ BD
  - Contrast limit: ΔH~10-13.5
- Locally-Optimized Combination of Images
  - LOCI is a least-squares minimization algorithm
  - Combines images to construct PSF that minimizes residuals
  - Lafreniere et al. 2007 ApJ 660

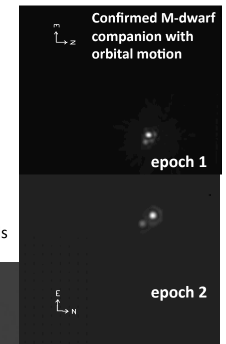

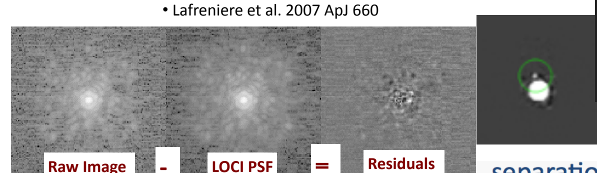

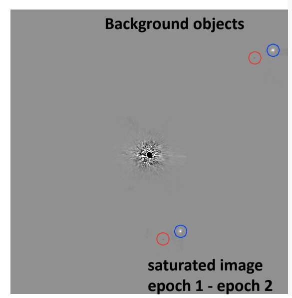

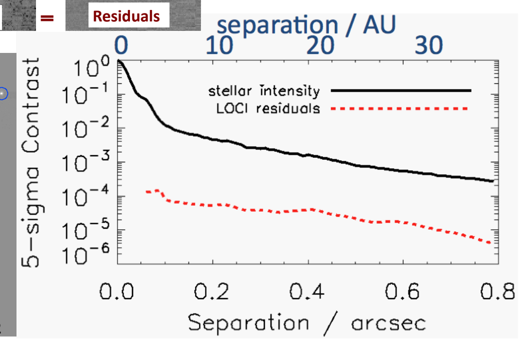

The Composition of Dwarfs in the Solar Neighborhood

Michael Pagano[1], Patrick Young[1], Frank Timmes[1], Jade Bond[2]

[1]Arizona State University [2]University of Arizona

Abstract

We analyze published elemental abundances derived from high-resolution spectroscopy from radial velocity planet searches. We find that the sun has anomalous abundances compared to compared to a uniform sample of nearby, >3Gyr old FGK dwarfs. Variations in this sample should primarily reflect differences in initial composition. We propose individual [element/Fe] ratios as a function of [Fe/H] for 13 elements. Scenarios for enrichment of outliers are discussed.

Introduction

The composition of the Sun has been generally taken to be a good representation of stars in the local neighborhood with a similar level of chemical enrichment, especially stars that would host exosolar planets. We attempt to determine mean abundances of several elements as a function of iron enrichment along with the dispersion of these abundances, using Bond et al.(2006,2008) high resolution data looking at 145 G stars, 29 of which have planets.

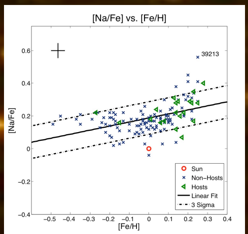

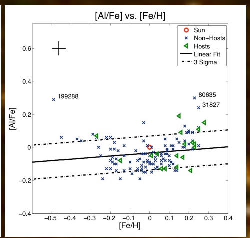

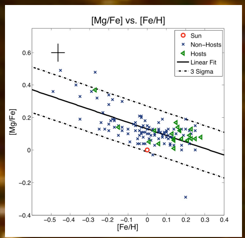

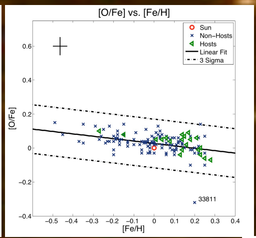

The Sun

Throughout this research we analyze the effect of updated solar compositions on the uniqueness of the sun. Bond(2006,2008) use initial solar compositions from Grevesse and Sauval,1998 (GS98); however we update the soar composition with data from Grevesse, Asplund, and Sauval, 2007 (GAS07), and Lodders et al. 2009 (L09). The elements Ca, Cr, and Ni differ by less than ten percent from the fitted value for [Fe/H] = 0. In all cases the solar value falls slightly below the fit for Ca and Cr, while for the revised compositions Ni is slightly overabundant in the sun. Ti varies from 10% to 25% depleted relative to the mean depending upon the Ti line used for the abundance determination and which initial solar abundance was used. Mg is similar to the local trend for all three solar compositions. C and Na are close to 20% deficient in the sun for the old values, but the new values place C more than 30% below the local mean. The Na value for the new compositions are significantly different, being 17% depleted for L09 values and 35% for GAS07. The L09 value agrees with the Na abundance determined from meteorites. Al is 8% overabundant for GAS07 15% for GS98, and 33% for L09. Si shows the largest deviation of all the elements relative to GS98, with the sun having a 30% deficit. For the new compositions the disparity is reduced to 18-20%. The solar O sits almost directly on the mean for GS98, but is depleted by 12 and 25%, respectively, for L09 and GAS07.

References and Acknowledgements

Arnett, David. Supernovae and Nucleosynthesis. Princeton University Press.
Bond, J.C. et al. 2006, MNRAS, 370, 163
Bond, J.C. et al. 2008, ApJ, 682, 1234
Ellinger, C., Young, P.A., Desch, S.J. 2009 ApJ submitted.
Grevesse, N., Asplund, M., \& Sauval, A. J. 2007, Space Sci. Rev., 130, 105.
Grevesse, N., \& Sauval, A. J. 1998, Space Sci. Rev., 85, 161.
Lodders, K., Palme, H., \& Gail, H. 2009, Landolt-Bornstein, New Series, Astronomy and Astrophysics. Berlin: Springer.
Young, P.A., Ellinger, C., Arnett, D., Fryer, C.L., Rockefeller, G. 2009, ApJ, 699, 938.
We would like to thank the NASA Astrobiology Institute and the ASU Astrobiology team for their support.

Element	Intrinsic Spread
C	±0.036
O	±0.048
Na	±0.033
Mg	±0.047
Al	±0.034
Si	±0.034
Ca	±0.033
TiI	±0.042
TiII	±0.043
Cr	±0.041
Ni	±0.035
Y	±0.047
Zr	±0.048
Ba	±0.049
Nd	±0.049
Eu	±0.052

Table 1. The abundance variation using GAS07 initial solar composition.

Abundance Patterns

First, we wish to know the mass fraction relative to solar so that we may construct abundances for stellar models that match the average composition of local stars.

There seems to be no one typical composition for stars in the solar neighborhood. There are identifiable trends for each element with Fe abundance, but there is a large variation about the mean as well as an interesting number of far outliers. This suggests an interesting history of chemical enrichment for the solar neighborhood beyond the mean field Galactic chemical evolution.

Element	Best Fit Equation for GS98	R^2	Intercept for Equation GAS07	LPG09	Deviation from Solar Abundance GS98	GAS07	LPG09
C	-0.108×Fe + 0.088	0.03	0.173	0.173	-0.088	-0.173	-0.173
O	-0.168×Fe + 0.008	0.08	0.121	0.051	0.008	-0.121	-0.051
Na	0.247×Fe + 0.090	0.21	0.188	0.068	-0.090	-0.188	-0.068
Mg	-0.262×Fe - 0.032	0.19	-0.019	-0.029	0.032	0.019	0.029
Al	0.092×Fe - 0.079	0.03	-0.034	-0.124	0.079	0.093	0.124
Si	0.114×Fe + 0.114	0.11	0.098	0.078	-0.114	-0.098	-0.078
Ca	-0.141×Fe + 0.020	0.08	0.027	0.027	-0.020	-0.027	-0.027
TiI	-0.402×Fe + 0.041	0.45	0.131	0.100	-0.041	-0.131	-0.100
TiII	-0.384×Fe - 0.025	0.54	0.065	0.035	0.025	-0.065	-0.035
Cr	0.045×Fe + 0.043	0.02	0.021	0.011	-0.043	-0.021	-0.011
Ni	0.146×Fe + 0.006	0.13	-0.031	-0.021	-0.006	0.031	0.021
Y	-0.15×Fe - 0.100	0.08	-0.112	-0.102	0.100	0.112	0.102
Zr	-0.308×Fe + 0.022	0.14	0.007	0.017	-0.022	-0.007	-0.017
Ba	-0.198×Fe - 0.054	0.05	-0.134	-0.144	0.054	0.134	0.144
Nd	-0.465×Fe + 0.040	0.27	0.064	0.044	-0.040	-0.064	-0.044
Eu	-0.530×Fe - 0.121	0.31	-0.154	-0.164	0.121	0.154	0.164

Table 2. The equations and intercepts for the best fit lines. Also the deviation of the sun from these lines.

Outliers

We denote any star that is significantly outside of three times the standard deviation for any abundance as an outlier. Table 3 shows the abundances for elements lighter than and including Ni for all the outliers. In this table the enhancement is given relative to the average abundance at the stellar [Fe/H] given by the fits in Table 2.These exceptional stars are worth our attention as they may preserve evidence of individual enrichment events.

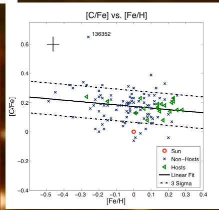

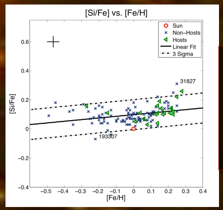

Elemental Abundance plots for Na, Al, Mg, C, O, and Si. The sun is indicated by an open circle. The least squares fit to the distribution is shown by the heavy solid line, and average observational errors are shown in the top left.

Star	[Fe/H]	Elemental Anomaly(X)	$[X/Fe]_{avg}$
HD208998	-0.290	Mg	**0.473**
HD23079(host)	-0.150	Cr	**0.285**
HD53705	-0.180	O	**0.601**
HD192865	0.020	Ni	**-0.262**
HD212708	0.180	Ni	**-0.265**
HD42902	0.220	Ni	**-0.171**
HD22104	0.200	Ni	**0.222**
HD193193	-0.040	Ca	**-0.643**
HD33811	0.200	Ca	**-0.319**
HD199288	-0.490	Al	**0.369**
HD80635	0.230	Al, Ni	**0.313, 0.178**
HD31827	0.250	Al, Si	**0.251, 0.183**
HD158783	0.000	Na	**-0.228**
HD39213	0.250	Na	**0.310**
HD136352	-0.260	C	**0.448**

Table 3. Outlier Abundances, given by the anomalous element and its variation from the average [X/Fe]

Lithium depletion in solar-like stars

Iván Ramírez

Baumann, Ramírez, Meléndez, Asplund, & Lind (2010, A&A, in press)

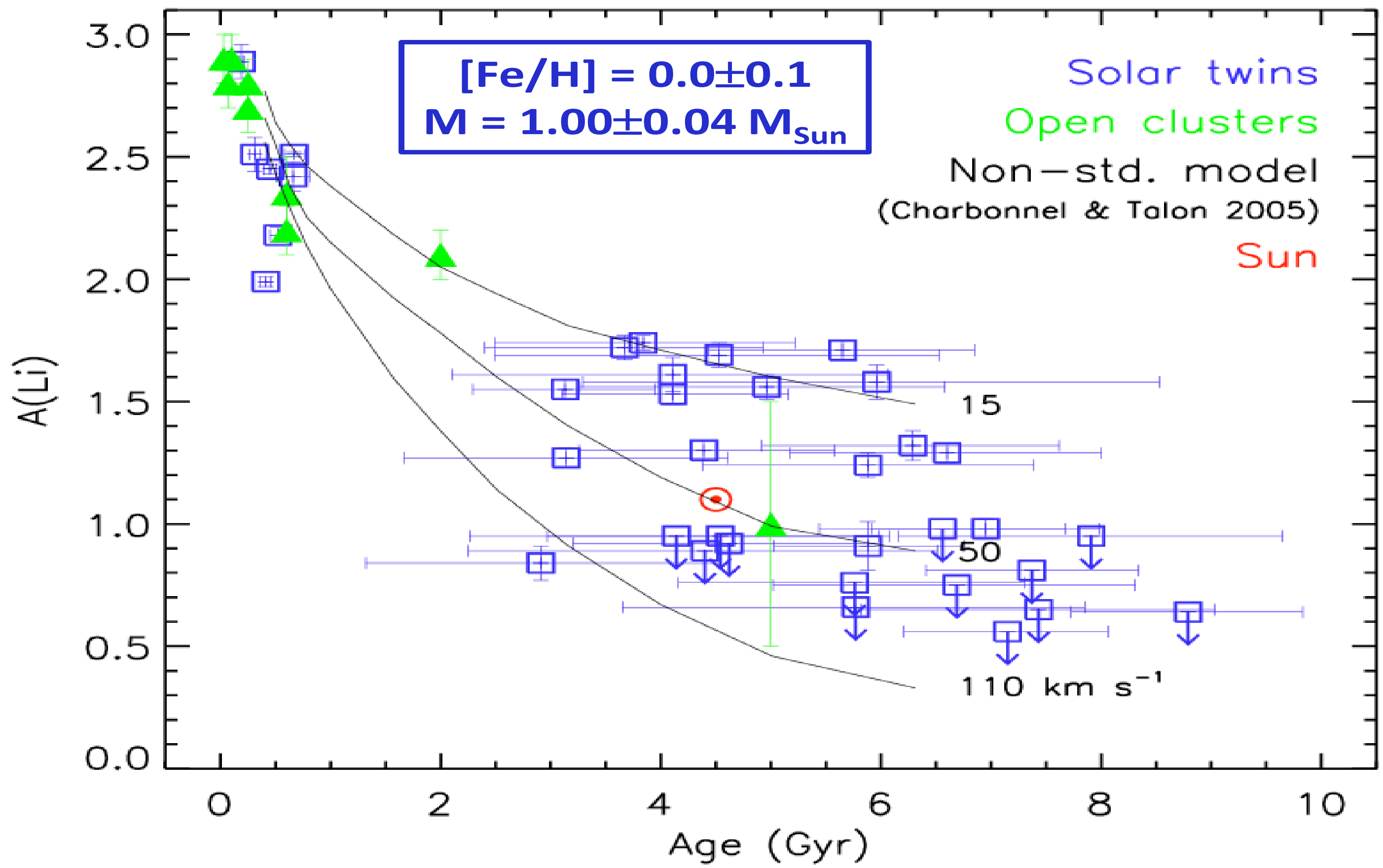

When restricted to a narrow range of mass and metallicity, solar-like stars follow a Li-age trend that can be explained by non-standard models of surface Li depletion.

The low solar Li abundance is normal for a star of its age, mass, and metallicity.

Ramses Ramirez
Department of Geosciences
Penn State University
email: rmr5265@psu.edu

Atmospheric escape and its role on Earth, Mars, and Extrasolar Planets

Jeans escape

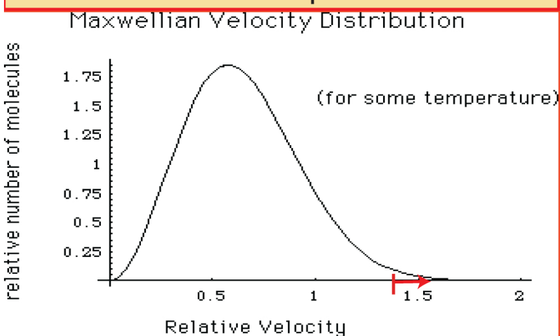

- Not effective for elements heavier than H or He

Hydrodynamic escape

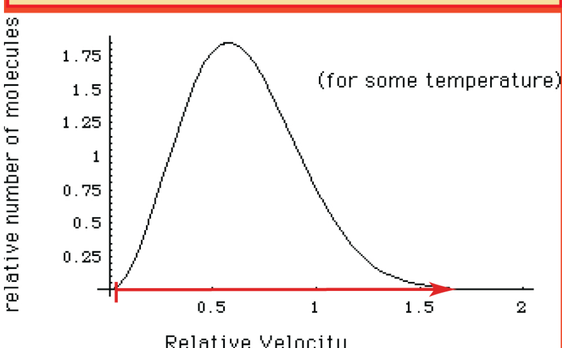

- Significant early on in solar system(high solar EUV)
- Heavier species can escape as well

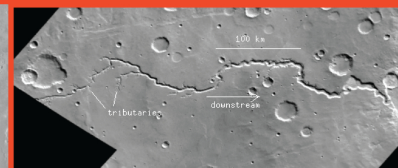

-The martian southern highlands (above) is home to many river valley systems

-The northern lowlands (left) consists of outflow channels and "chaos terrain"

- This suggests Mars had a thicker atmosphere and a much warmer, wetter climate

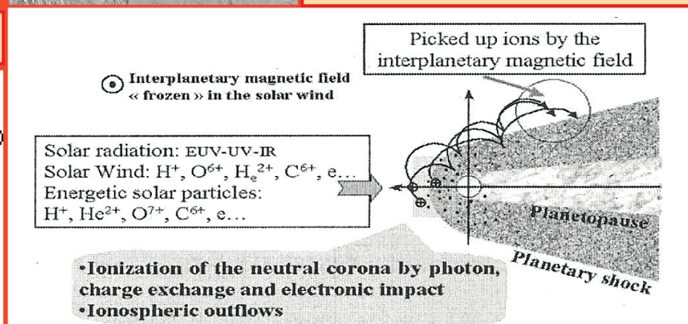

-Important on Mars after LHB ends and EUV negligible. After magnetic field is lost ~3.7 bya, 3 non-thermal mechanisms dominate:

Photochemical escape(dissociative recombination)
Sputtering: Particles picked by solar wind reimpact atmosphere, inducing ejection
Ion pick up: Direct ion loss due to solar wind acceleration

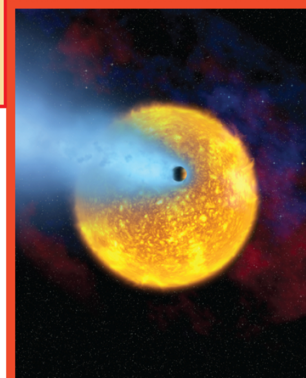

- A **Chtonian planet** is the remaining rocky or metallic core resulting from the stripping away of a gas giant's hydrogen and helium layers via hydrodynamic escape

- The result resembles a terrestrial planet

-COROT-7b (above) is probably the first such planet.

- HD 209458 b (above) was the first among various categories:
  first transiting extrasolar planet discovered
  first extrasolar planet known to have an atmosphere
  first extrasolar planet observed to have an evaporating H atmosphere
  first extrasolar planet found to have an atmosphere containing carbon and oxygen